arXiv:1610.07526v2 [hep-ph] 14 Nov 2016

Implication of the ALEPH 30 GeV dimuon resonance at the LHC

P. Ko*

School of Physics, KIAS, Seoul 02455, Korea and

Quantum Universe Center, KIAS, Seoul 02455, Korea

Jinmian Li†

School of Physics, KIAS, Seoul 02455, Korea

Chaehyun Yu‡

Department of Physics, Korea University, Seoul 02841, Korea

(Dated: November 15, 2016)

Abstract

Recent reanalysis of ALEPH data on $Z \to b\bar{b} + X$ seems to indicate an existence of the dimuon excess around 30 GeV with a branching fraction for $Z \to b\bar{b}\mu^+\mu^-$ around 1.1×10^{-5}. In this letter, we discuss three different types of simplified models for this possible excess. In the first class of models, we assume a new resonance couples to both $b\bar{b}$ and $\mu^+\mu^-$. Within the allowed parameter space for the ALEPH data, this type of models is excluded because of too large Drell-Yan production of dimuon from the $b\bar{b}$ collision at the LHC. In the second model, we assume that the 30 GeV excess is a new gauge boson Z' that couples to the SM b and a new vectorlike singlet B quark heavier than Z and not to $b\bar{b}$. Then one can account for the ALEPH data without conflict with the DY constraint. The new vectorlike quark B can be pair produced at the LHC 8/13 TeV by QCD with $\sigma(BB) \sim O(100 - 1000)$ pb, and Bq production rate is $\sigma(Bq) \sim$ a few pb which is larger than $\sigma(Bb)$ roughly by an order of magnitude. Their signatures at the LHC would be $2b + 4\mu$, $bj + 2\mu$ and $2b + 2\mu$, respectively, which however might have been excluded already by LHC run I and II data since the multi-muon events have low SM background and are rare at the LHC. Finally we consider $Z \to Z'\phi$ followed by $Z' \to \mu^+\mu^-$ and $\phi \to b\bar{b}$ assuming that the Higgs field for Z' mass is also charged under the SM $U(1)_Y$ gauge symmetry. In this class of model, we could accommodate the $\mathrm{Br}(Z \to b\bar{b}\mu^+\mu^-) \sim 1.1 \times 10^{-5}$ if we assume very large $U(1)'$ charge for the $U(1)'$ breaking Higgs field.

PACS numbers:

*pko@kias.re.kr

†jmli@kias.re.kr

‡chyu@korea.ac.kr

I. INTRODUCTION

A recent reanalysis of the archived ALEPH data on $Z \to b\bar{b} + X$ might suggest an interesting possibility of a new resonance X with mass 30 GeV decaying into $\mu^+\mu^-$ [1]:

$$\mathrm{Br}(Z \to b\bar{b}\mu^+\mu^-) \sim 1.1 \times 10^{-5}, \tag{1}$$

$$\Gamma_{\mathrm{tot}}(X) = (1.78 \pm 1.14)\ \mathrm{GeV}. \tag{2}$$

Dielectron channel also shows some excess, which however is less prominent than the dimuon channel. The $\cos\theta^*_\mu$ distribution of a muon in the rest frame of dimuon system with respect to the direction of the dimuon system in the rest frame of Z shows peaks around $\cos\theta^*_\mu \approx \pm 1$, which would prefers X being a spin-1 particle.

In this letter, we consider three types of simplified models for this 30 GeV dimuon excess, for which the relevant Feynman diagrams are shown in Fig. 1 (a)–(c). Note that these three types of Feynman diagrams exhaust all possible tree-level mechanisms for this dimuon excess.

In Sec. II, we assume a new resonance X couples to both $b\bar{b}$ and $\mu^+\mu^-$ with X being (pseudo)scalar or (axial) vector boson, as shown in Fig. 1(a). Then we perform comprehensive phenomenological study on $X \to b\bar{b}\mu^+\mu^-$ and related processes such as $X \to 4\mu, 4b$, finding out the parameter space that can account for the ALEPH data. Then within this parameter space, we study the predictions involving X at the LHC: Drell-Yan (DY) process from $b\bar{b} \to X \to \mu^+\mu^-$, and X productions in $t \to bWX$, $b\bar{b}X$ and $t\bar{t}X$ at the LHC. Our finding is that the DY production of dimuon basically rules out this class of models shown in Fig. 1(a). Then in Sec. III, we propose a model that can evade the strong constraint from the DY. Here we introduce a new vectorlike down-type singlet quark (B) and assume the dimuon resonance X is a spin-1 particle Z'. The relevant diagram is shown in Fig. 1(b). Assuming that only Z-b-B, Z'-b-B and Z'-μ-μ couplings are nonzero, we can identify the parameter space compatible with the ALEPH 30 GeV dimuon excess. Then we discuss the LHC phenomenology of B quarks, calculating its production cross sections and identifying the final states. In Sec. IV, we consider a model with a new $U(1)'$ gauge symmetry with the associated gauge boson Z' and the singlet scalar boson ϕ charged under $U(1)_Y \times U(1)'$. From the nonzero value of Z-Z'-ϕ vertex, one can account for $Z \to Z'\phi \to \mu^+\mu^- b\bar{b}$ without conflict with any known experimental constraints, but we need a very large $U(1)'$ charge for the $U(1)'$ breaking Higgs field. Finally we will summarize the results in Sec. V.

II. SIMPLIFIED MODELS–I

For a resolution of the 30 GeV dimuon excess, we introduce a new particle X, which could be one of scalar (s), pseudoscalar (a), vector (V), or axial vector (A). We assume that

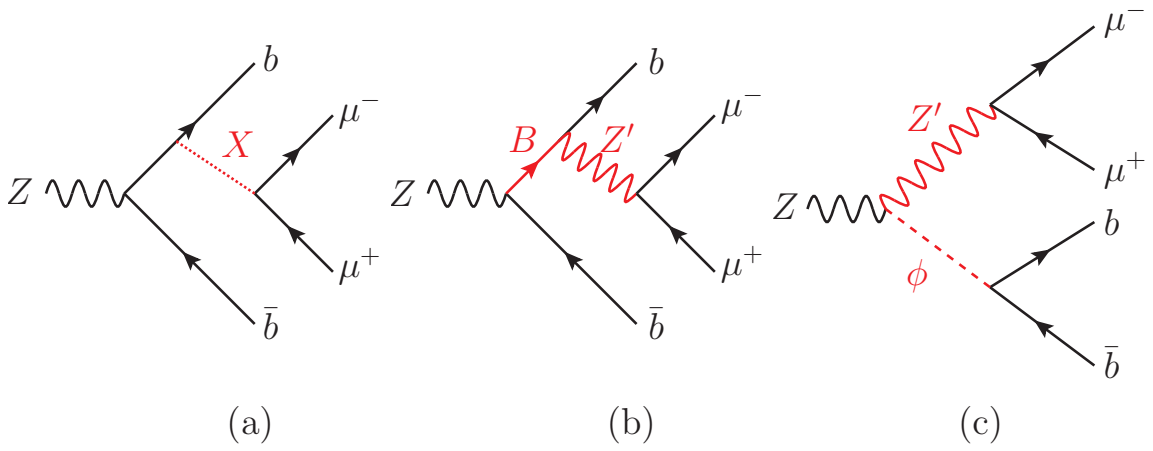

FIG. 1: Feynman diagrams for the $Z \to b\bar{b}\mu^+\mu^-$ decay.

the interaction Lagrangian is one of the following forms for $X = s, a, V, A$:

$$\mathcal{L}_{\text{scalar}} = s \sum_f g_f^s \bar{f} f, \tag{3a}$$

$$\mathcal{L}_{\text{pseudoscalar}} = ia \sum_f g_f^a \bar{f} \gamma_5 f, \tag{3b}$$

$$\mathcal{L}_{\text{vector}} = -V_\mu \sum_f g_f^V \bar{f} \gamma^\mu f, \tag{3c}$$

$$\mathcal{L}_{\text{axial vector}} = -A_\mu \sum_f g_f^A \bar{f} \gamma^\mu \gamma_5 f. \tag{3d}$$

We consider only two couplings are nonzero: g_μ^X and g_b^X for $X = s, a, V, A$. In the pseudoscalar and axial vector cases, the phenomenology for the Z decay and LHC phenomenology are similar to the scalar and vector cases, respectively. Hereafter, we discuss the latter cases unless there is significant change in the former cases. For the numerical analysis, we use MadGraph5 [2] with implementing the models, Eqs. (3).

Then X mainly decays into a $b\bar{b}$ or $\mu^+\mu^-$ pair. The decay width of X (Γ^X) depends on both g_μ^X and g_b^X. We find that the X boson has a very narrow width for small couplings. For example, $\Gamma^V = 3 \times 10^{-3}$ (0.3) GeV for $g_\mu^V = g_b^V = 0.03$ (0.3) and $\Gamma^s = 4 \times 10^{-3}$ (0.4) GeV for $g_\mu^V = g_b^V = 0.03$ (0.3), respectively. In order to achieve a large decay width, $\Gamma^X \sim 1$ GeV, the couplings should be about $g_f^V \sim 0.6$ or $g_f^s \sim 0.5$, respectively. If there are other decay channels, the decay width could be enhanced. However if the decay channels to light quarks or e^+e^- are open, much more stringent constraints on the model would be encountered. Thus one must consider smaller couplings to the light quarks and electron, which mean that the X must be flavor-dependent. Another possibility would be the X decay into extra fermions or dark matter candidates, which often exist in UV complete models with flavor-dependent gauge interactions [3]. The extra decay channels would be model-dependent and the UV completion of the model is out of scope of this paper. In this section, we shall assume that the $X \to b\bar{b}, \mu^+\mu^-$ decay are the only possible decay channels for simplicity.

Since the X boson couples to b and μ, the couplings, g_b^X and g_μ^X can be constrained by the $Z \to 4b$ and $Z \to 4\mu$ decays, respectively. The branching ratio of the $Z \to 4b$ decay is

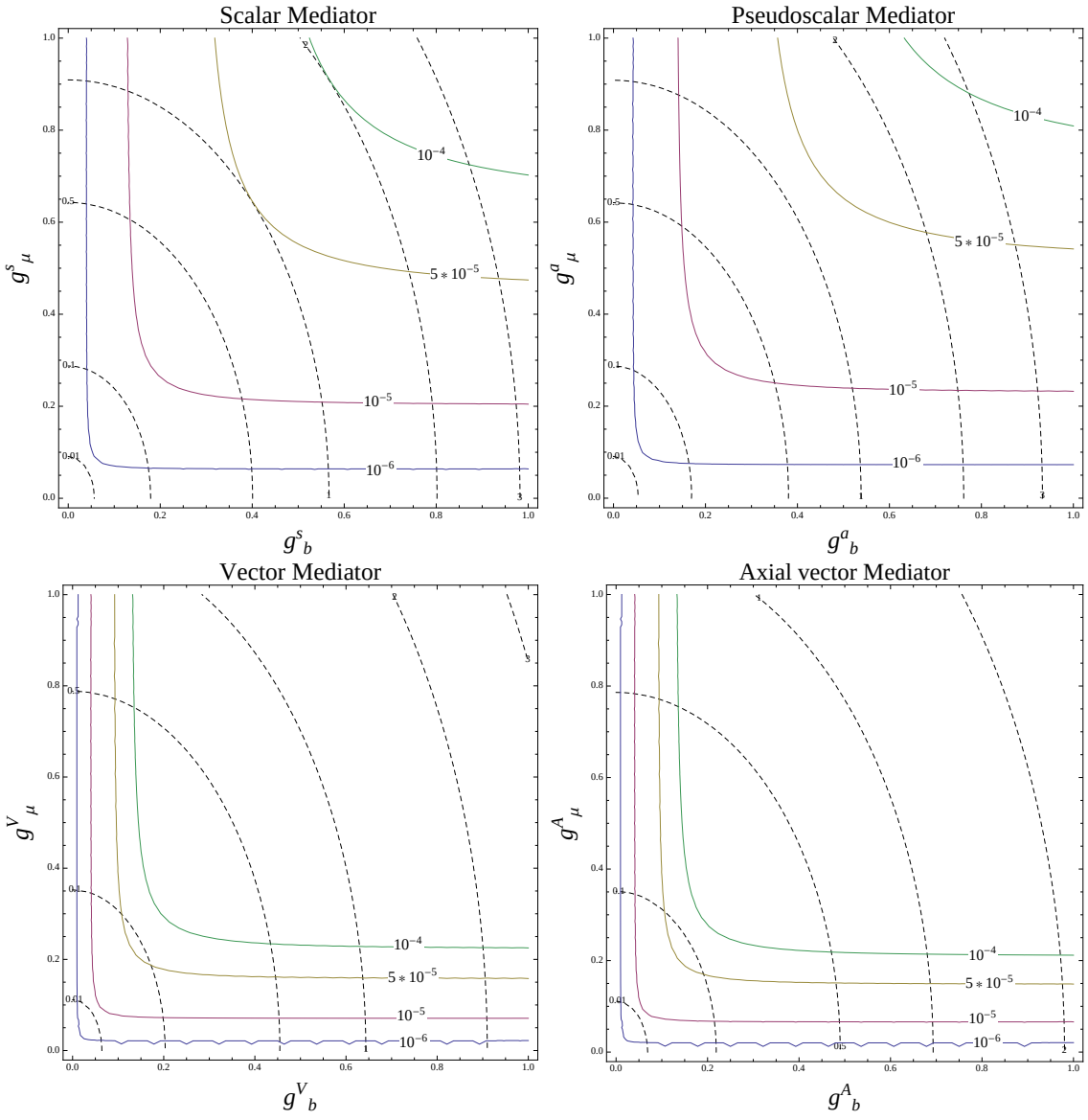

FIG. 2: Contour plots for g_b^X and g_μ^X. The solid lines correspond to $\Gamma^X(Z \to b\bar{b}\mu^+\mu^-)$ in unit of GeV while the dashed lines to the sum of $\Gamma(X \to b\bar{b})$ and $\Gamma(X \to \mu^+\mu^-)$ in unit of GeV.

$(3.6 \pm 1.3) \times 10^{-4}$ [4], whose uncertainty corresponds to $\Delta_{4b} = 3.3 \times 10^{-4}$ GeV. We find that the enhancement of the decay width for the $Z \to 4b$ is less than 3×10^{-4} GeV for $g_b^V \lesssim 0.5$ and $g_b^s \lesssim 0.7$, respectively, which imply that a little bit large couplings are not excluded by the $Z \to 4b$ decay. However, the $Z \to 4\mu$ decay might constrain this model significantly. The branching ratio of the $Z \to 4\ell$ (ℓ = either e or μ) decay was reported by the CMS and ATLAS collaborations at $\sqrt{s} = 7$, 8, and 13 TeV [5]. By the recasting the ATLAS search, the bound on g_μ^V is obtained as $g_\mu^V \lesssim 0.025 \sim 0.03$ for $m_V = 30$ GeV in the $L_\mu - L_\tau$ gauge model [6]. However, the bound strongly depends on the model, in particular, the total decay width of X. For more exact bound, the detailed analysis which would depend on the complete model and information on cuts in experiments is required.

In Fig. 2, we present the contour plots for the couplings, g_b^X and g_μ^X for $X = s$, a, V, and

$g_b^{Z'}$	$g_\mu^{Z'}$	$\Gamma^{Z'}(Z \to bb\mu\mu)$	$\Gamma(Z' \to bb, \mu\mu)$
0.1	0.1	2.72×10^{-5}	0.0322
$\sigma(pp \to Z' \to \mu\mu)$	$\Gamma(t \to bWZ')$	$\sigma(pp \to bbZ')$	$\mathrm{Br}(Z' \to \mu\mu)$
714.5 pb	1.267×10^{-4}	136.1 pb	0.25

TABLE I: Benchmark point I (vector mediator) at 13 TeV LHC.

$g_b^{Z'}$	$g_\mu^{Z'}$	$\Gamma^{Z'}(Z \to bb\mu\mu)$	$\Gamma(Z' \to bb, \mu\mu)$
0.7	0.1	3.036×10^{-5}	1.19
$\sigma(pp \to Z' \to \mu\mu)$	$\Gamma(t \to bWZ')$	$\sigma(pp \to bbZ')$	$\mathrm{Br}(Z' \to \mu\mu)$
920.5 pb	0.0062	6645 pb	0.0068

TABLE II: Benchmark point II (vector mediator) at 13 TeV LHC.

A, respectively. The solid lines represent the decay width of the $Z \to b\bar{b}X$ (or $Z \to \mu^+\mu^- X$) decay with subsequent decay $X \to \mu^+\mu^-$ ($X \to b\bar{b}$) in unit of GeV, which is denoted by $\Gamma^X(b\bar{b}\mu^+\mu^-)$, while the dashed lines to the sum of the decay widths of the $X \to b\bar{b}$ and $X \to \mu^+\mu^-$, which is approximately equal to the total decay width of the X boson. There are other diagrams in the SM, which interfere with the X-mediated diagrams. We find that the interference effects are negligible because the dimuon excess occurs near the X resonance and its decay width is quite narrow. The required decay width for the 30 GeV dimuon excess is $\Gamma^X(b\bar{b}\mu^+\mu^-) \sim 2.7 \times 10^{-5}$ GeV. In the cases of the scalar and pseudoscalar mediator, a little large couplings of about $g_\mu^{s,a} \sim g_b^{s,a} \sim 0.4$ are required to achieve the dimuon excess at ALEPH. In this region, the total decay width of the s (a) is about $0.5 \sim 0.7$ GeV, which is marginally consistent with the observed one within the 1σ level. We note that it is possible to achieve $\Gamma^{s,a} \sim 1.7$ GeV for $g_\mu^{s,a} \sim 0.7$ or $g_b^{s,a} \sim 0.7$ while satisfying the required decay width for $Z \to b\bar{b}\mu^+\mu^-$. In the cases of the vector and axial vector mediators, we find that the required decay width for the dimuon excess could be achieved for $g_\mu^{V,A} \sim g_b^{V,A} \sim 0.015$, but the total decay width of the $V(A)$ is much smaller; $\Gamma^{V,A} \sim 0.05$ GeV. We note that $\Gamma^{V,A} \sim 1$ GeV with the required decay width for the dimuon excess is possible for $g_\mu^{V,A} \sim 0.01$ and $g_b^{V,A} \sim 0.7$, but this region would be excluded by the $Z \to 4b$ decay.

Next, we consider some phenomenology of the vector-mediator model at the LHC with $\sqrt{s} = 13$ TeV. Now we call the V as a Z' boson. Since the Z' couples with b quark and μ, the processes which include both or either of b or μ would provide stringent constraints. Among them, we investigate three processes: the Drell-Yan process, $pp \to Z' \to \mu^+\mu^-$, the top decay, $t \to bWZ'$, and the Z' production associated with a $b\bar{b}$ pair, $pp \to b\bar{b}Z'$.

Here, we consider two benchmark points. In Table I, the couplings are taken to be $g_\mu^{Z'} = g_b^{Z'} = 0.1$, which yield $\Gamma^{Z'}(Z \to bb\mu\mu) = 2.72 \times 10^{-5}$ GeV. Since the branching ratio of $Z' \to \mu\mu$ is 0.25, the cross section for $pp \to bbZ'$ with the subsequent decay $Z' \to \mu\mu$ would be about 34 pb, which can be a probe of this model. For the top decay, the branching ratio of $t \to bWZ'$ followed by $Z' \to \mu\mu$ would be about 2×10^{-5}, which could be another probe at the LHC. The most significant process is the Drell-Yan process, whose cross section is about 715 pb, which is already excluded by the CMS data [7].

In Table II, we take the couplings to be $g_\mu^{Z'} = 0.1$ and $g_b^{Z'} = 0.7$, which yield $\Gamma^{Z'}(Z \to bb\mu\mu) = 3.04 \times 10^{-5}$ GeV. As we already discussed, this set would be excluded because it predicts a large decay width for $Z \to 4b$ via the Z' exchange. Actually, the decay width

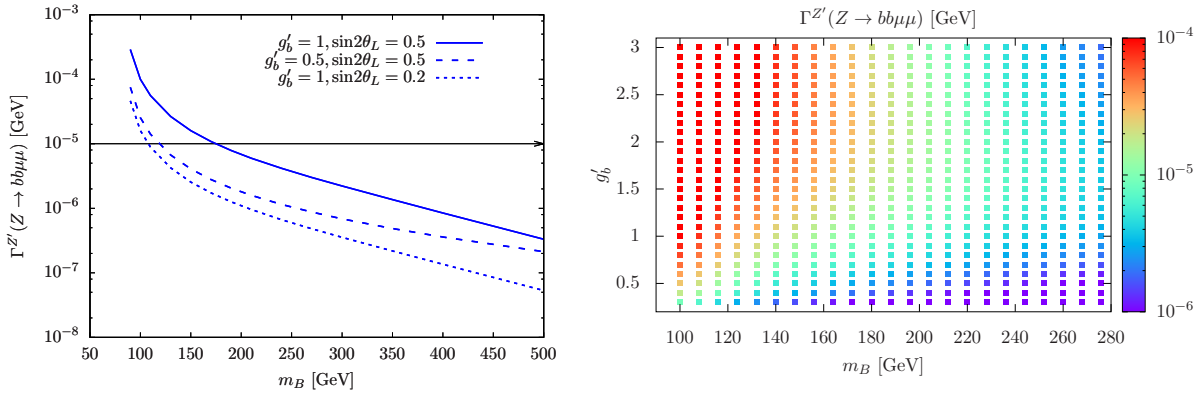

FIG. 3: The $\bar{b}b\mu\mu$ partial decay width of the Z boson from new physics contribution. $\sin\theta_L = 0.5$ in the right panel.

is about 1.7×10^{-3} GeV, which is much larger than the PDG value. The cross section for $pp \to bbZ'$ is about 6600 pb and, then, it for $pp \to bbZ'$ followed by $Z' \to \mu\mu$ is about 45 pb, which can be easily proved at the LHC. In this case, the Drell-Yan process strongly constrains this model, too. The predicted cross section reach about 900 pb, which is already excluded by the CMS data [7].

We also investigate some benchmark points in the scalar-mediator model. We find that the cross section for the Drell-Yan cross section exceed 380 pb at $\sqrt{s} = 13$ TeV for $g_b^s = g_\mu^s = 0.1$, which is also excluded by the CMS data. We note that those couplings are too small to provide the required decay width for the dimuon excess.

Since the X boson can couple to both $b\bar{b}$ and $\mu^+\mu^-$ in the models discussed in this section, one may observe a similar peak of the X boson for the invariant mass of the bb pair, depending on the couplings of the X . So far the $b\bar{b}$ peak in $Z \to b\bar{b}\mu^+\mu^-$ has not been observed in the Z decay yet. The search for the resonance of the $b\bar{b}$ pair would be another probe of those models.

Summarizing this section, we investigated some benchmark points to predict the required decay width for the ALEPH 30 GeV dimuon excess reported in Ref. [1] in simplified models defined by Eqs. (3a)–(3d) and Fig. 1(a). In general, one can find the preferred points, but they predict too large cross sections or branching ratios in other productions or decay channels. Most notably the Drell-Yan process turns out to be the most stringent constraints, and the simplest benchmark points (and also other points) are easily excluded by the LHC data, in particular, by the Drell-Yan process. One might decrease the Drell-Yan cross section by increasing the decay width of X, but it necessarily decreases the decay width for $Z \to bb\mu\mu$ and the dimuon excess would not be explained with the X boson with interactions defined in Eqs. (3a)–(3d).

III. SIMPLIFIED MODEL–II

The Model-I in Sec. II has a problem with DY production through $b\bar{b} \to Z' \to \mu^+\mu^-$. One can avoid this problem by making Z' decouple from $b\bar{b}$ and introducing a new vectorlike down-type quark B which has a nonzero Z-b-B and Z'-b-B couplings.

Let us assume a down-type vectorlike singlet quark B with the following interactions (see

g'_b	m_B	$\Gamma^{Z'}(Z \to bb\mu\mu)$	$\Gamma(B \to bZ')$
0.7	110 GeV	2.75×10^{-5}	3.4 GeV
$\mathrm{Br}(B \to bZ')$	$\sigma^{13}(BB)/\sigma^{8}(BB)$	$\sigma^{13}(bB)/\sigma^{8}(bB)$	$\sigma^{13}(qB)/\sigma^{8}(qB)$
1.0	3942/1203 pb	1.68/0.89 pb	7.49/3.2 pb

TABLE III: Benchmark point III (vectorlike particle model).

g'_b	m_B	$\Gamma^{Z'}(Z \to bb\mu\mu)$	$\Gamma(B \to bZ')$
2.0	180	2.35×10^{-5} GeV	124.4 GeV
$\mathrm{Br}(B \to bZ')$	$\sigma^{13}(BB)/\sigma^{8}(BB)$	$\sigma^{13}(bB)/\sigma^{8}(bB)$	$\sigma^{13}(qB)/\sigma^{8}(qB)$
1.0	391/120 pb	0.21/0.1 pb	4.24/1.67 pb

TABLE IV: Benchmark point IV (vectorlike particle model).

Ref. [8]):

$$\mathcal{L} = g'_\mu Z'_\rho \bar{\mu}\gamma^\rho \mu + g_s G^a_\mu \bar{B}\gamma^\mu T^a B - \left[\frac{1}{2} g'_b Z'_\rho \bar{b}\gamma^\rho B + \frac{g_W \sin 2\theta_L}{4c_W} Z_\mu \bar{b}\gamma^\mu P_L B + h.c.\right]. \quad (4)$$

Here the Z' coupling to the quark sector is assumed to always involve the vectorlike quarks so that $Z' \to b\bar{b}$ is zero (or highly suppressed) and the DY process is not allowed (or highly suppressed).

The ALEPH 30 GeV dimuon excess in the Z decay is explained by $Z \to bB^* \to bb\mu^+\mu^-$ assuming that B is heavier than Z so that $Z \to B\bar{b} + C.C.$ involves a virtual B quark. The main decay channels of B would be $B \to bZ'$. As for Z', we assume that the $Z' \to \mu^+\mu^-$ is the only kinematically allowed decay channel, so the g'_μ parameter is not relevant to the partial decay width of $Z \to bB^* \to bb\mu^+\mu^-$ decay and will be set to $g'_\mu = 0.01$ according to the $Z \to 4\mu$ measurement [6].

In Fig. 3, we show the partial width of $Z \to bB^* \to bb\mu^+\mu^-$ ($\Gamma^{Z'}(Z \to bb\mu\mu)$) in terms of the parameters of the Model-II, i.e. m_B, g'_b and $\sin 2\theta_L$. From the left panel of Fig 3, we can observe the $\sin^2 2\theta_L$ behavior of $\Gamma^{Z'}(Z \to bb\mu\mu)$, while the dependence on g'_b is more complicate because it could change the total width of B which is important for $\Gamma^{Z'}(Z \to bb\mu\mu)$. So in the right panel, fixing $\sin\theta_L = 0.5$, we show the $\Gamma^{Z'}(Z \to bb\mu\mu)$ in the 2-dimensional plane of g'_b and m_B. From the figure, we can find the ALEPH dimuon excess can be addressed in the parameter space with $m_B \sim 100 - 200$ GeV, $g'_b \sim 0.5 - 3$ and $\sin\theta_L \sim 0.5$, requiring that g'_b remains within the perturbative regime.

Two benchmark points with appropriate dimuon excess and different masses for the vectorlike B are given in Table III and Table IV. For the relatively heavy B, a coupling g'_b that approaches the perturbativity limit ($g'_b = 2$) is required, rendering very large decay width of B whose main decay channel is assumed to be $b\mu\mu$. It will be important to study the signals of those two benchmark points at the LHC. The process with the largest cross section is the pair production of $B\bar{B}$ through QCD coupling, followed by the $B \to bZ'$ decay which produces the $bb + 4\mu$ signal. The corresponding production cross section at the 13/8 TeV LHC for benchmark points ($\sigma^{13}(BB)/\sigma^{8}(BB)$) are given in the Tables III and IV for $m_B = 110$ GeV and 180 GeV, respectively. The cross section is quite sensitive to the mass of B, raising the m_B from 110 GeV to 180 GeV can reduce the cross section by one order of magnitude. Even though there is no LHC search for $bb + 4\mu$ final states so far, the signal

is almost background free and $b\bar{b}$ + multi muon events are rare. Therefore it is very likely that this kind of model has been excluded already [9].

Because of the b-B-Z coupling, there could also be signals of $pp \to Z \to bB$ and $qb \to qB$ with $t-$channel Z exchange, where $q = u, d, s, c$. These processes will generate the signal of $b\mu\mu$ that is associated with an additional b-jet or light flavor jet, the cross sections of which are proportional to $\sin^2 2\theta_L$. Those cross section for benchmark points are also presented in Table III and Table IV, where we find both processes have production cross section of $\mathcal{O}(1)$ pb at the 13/8 TeV LHC and t-channel process has much larger production rate than the s-channel process. Moreover, as we can expect, the production cross section of the $t-$channel process is less sensitive to m_B than that of the $s-$channel process. It would be highly desirable to look into $bb + 4\mu$, $bb + 2\mu$, and $bj + 2\mu$ more carefully at the LHC and test this model for the ALEPH 30 GeV dimuon excess.

IV. NEW GAUGE $U(1)'$ MODEL

In this section, we introduce a model with new $U(1)'$ gauge symmetry, which includes a new gauge boson Z' and a new real scalar ϕ (see Fig. 1(c)). Here, we do not focus on the details of this model, but we just mention that the $U(1)'$ could be the $U(1)_{L_\mu - L_\tau}$ where $Z' \to e^+e^-$ can be naturally suppressed. The scalar ϕ is assumed to be charged under both $U(1)_Y$ and $U(1)'$ gauge groups, with their charges being Y_ϕ and Y'_ϕ, respectively. The $U(1)'$ is spontaneously broken by the nonzero VEV of ϕ, v_ϕ. Since ϕ is charged under $U(1)_Y \times U(1)'$ gauge symmetries, there appear three neutral spin-1 fields, B_μ, W^3_μ, and $\hat{Z}'_\mu$, which are mixed with each other after electroweak and $U(1)'$ symmetry breaking. Then one can obtain three mass eigenstates, A_μ (massless photon), Z_μ, and Z'_μ. Given that the covariant derivative for ϕ is written as

$$D_\mu \phi = \partial_\mu \phi - i g_1 Y_\phi B_\mu \phi - i g' Y'_\phi Z'_\mu \phi,$$

one can write down the mass matrix for three neutral gauge bosons in the interaction eigenstates, $(B_\mu, W^3_\mu, \hat{Z}'_\mu)$ as

$$M_V^2 = \begin{pmatrix} g_1^2 \frac{v^2}{8} + g_1^2 Y_\phi^2 v_\phi^2 & -g g_1 \frac{v^2}{8} & g_1 g' Y_\phi Y'_\phi v_\phi^2 \\ -g g_1 \frac{v^2}{8} & g^2 \frac{v^2}{8} & 0 \\ g_1 g' Y_\phi Y'_\phi v_\phi^2 & 0 & g'^2 Y'^2_\phi v_\phi^2 \end{pmatrix}, \tag{5}$$

where g_1, g, and g' are the couplings of the $U(1)_Y$, $SU(2)_L$, and $U(1)'$, respectively.

We shall simply assume the $U(1)'$ gauge symmetry is related to the μ–flavor so that Z' can dominantly decay into $\mu^+\mu^-$. On the other hand the scalar ϕ would decay mainly into $b\bar{b}$ through its mixing with the SM Higgs boson, with the Yukawa coupling given by

$$\frac{m_b}{v} \sin\alpha \sim \frac{1}{50} \sin\alpha \lesssim 10^{-3}.$$

We have used the fact that the current bound on the singlet-Higgs mixing angle (α) from the 125 GeV Higgs signal strengths is $\sin\alpha \lesssim 0.4$ depending on the ϕ mass [10, 11].

The following constraints have to be applied to be consistent with experimental measurements in order that we try to explain the dimuon excess:

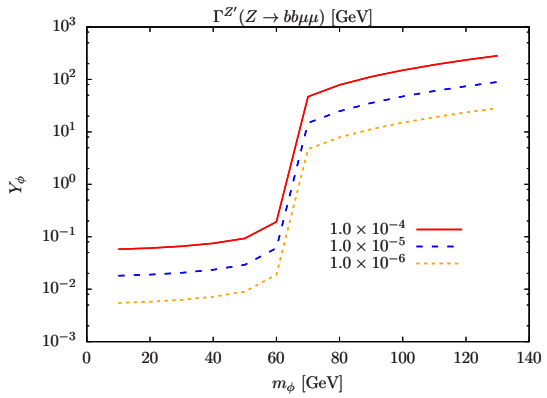

FIG. 4: The contours of $\Gamma^{Z'}(Z \to bb\mu\mu)$ with varying m_ϕ and Y_ϕ. The dimuon excess requires $\Gamma^{Z'}(Z \to bb\mu\mu) \sim 2 \times 10^{-5}$ GeV.

- The mixing between Z' and SM gauge field should be small, so we have $(M_V^2)_{33} \sim \frac{1}{2} m_{Z'}^2$ where $m_{Z'} \sim 30$ GeV according to the observed excess. Then, we can express $v_\phi = \frac{m_{Z'}}{\sqrt{2} g' Y'_\phi}$.

- The current measurements imply the mixing between Z' and SM Z to be $\sin\theta_{ZZ'} \lesssim \mathcal{O}(10^{-2}) \sim \mathcal{O}(10^{-3})$ [12] and the mixing between Z' and photon to be $\sin\theta_{\gamma Z'} \lesssim \mathcal{O}(10^{-2})$ [13] for $m_{Z'} = 30$ GeV. This requires very small off-diagonal component of the gauge boson mass matrix, e.g. $(M_V^2)_{13} < 5$ GeV^2, which corresponds to $\sin\theta_{ZZ'} < 5.1 \times 10^{-4}$ and $\sin\theta_{\gamma Z'} < 9.8 \times 10^{-3}$ result in $\frac{Y_\phi}{Y'_\phi} \lesssim 3.2 \times 10^{-2} g'$.

- As we have discussed in Sec. II, the g' should be $g' \lesssim 0.02$ in order to suppress the $Z \to 4\mu$ decay. Then we find the condition for the ratio of $U(1)$ charges, $\frac{Y'_\phi}{Y_\phi} \gtrsim 1575$, which implies a large gap between two $U(1)$ charges or $Y_\phi = 0$.

- The Z-Z'-ϕ coupling is $C_{ZZ'\phi} = \frac{g_1}{\sqrt{g_1^2+g^2}} 2 g_1 Y_\phi m_{Z'} + \sin\theta_{ZZ'} \sin\alpha \frac{m_Z^2}{v}$, where only Y_ϕ is the free parameter. Taking $\sin\theta_{ZZ'} = 5.1 \times 10^{-4}$ (correspond to $(M_V^2)_{13} = 5$ GeV^2) and $\sin\alpha = 0.2$, we plot the contours of $\Gamma(Z \to bbZ')$ on the m_ϕ-Y_ϕ plane in Fig. 4. Assuming $\mathrm{Br}(Z' \to \mu\mu) = 100\%$, Y_ϕ in very large range of $\mathcal{O}(10^{-2}) - \mathcal{O}(10^2)$ can explain the dimuon excess.

- Finally $\phi \to b\bar{b}$ will occur through $\phi - h$ mixing, whose mixing angle $\sin\alpha$ is constrained to be $\sin\alpha \lesssim 0.2$ by the present LHC data on the Higgs signal strengths. Including the Yukawa coupling of the SM Higgs to the SM fermions, ϕ-b-$\bar{b}$ will be given by $(m_b/v)\sin\alpha \sim (1/50)\sin\alpha$.

In this model, we find that a very large $U(1)'$ charge for the scalar ϕ is required in order to accommodate the observed dimuon excess. For a reasonable hypercharge, say $Y_\phi \sim 1$, the required value for Y'_ϕ is $\mathcal{O}(10^4)$. This implies that a reasonable or natural model building for the $U(1)'$ model might be difficult to be accommodated with the dimuon excess.

The mixing of the Z and Z' may also be generated by the kinetic mixing, $\frac{\varepsilon}{2c_W} \hat{B}_{\mu\nu} \hat{Z}'^{\mu\nu}$ [14]. Assuming no mass mixing ($Y_\phi = 0$) for simplicity, we find that the coupling related to the

Z boson decay is

$$C_{ZZ'\phi} = (\sin\xi - \varepsilon t_W \cos\xi)\sqrt{2} g' Y'_\phi m_{Z'} + \sin\xi \sin\alpha \frac{m_Z^2}{v}, \tag{6}$$

with the mixing angle $\tan 2\xi = \frac{2\varepsilon t_W}{1-(\varepsilon t_W)^2 - m_{Z'}^2/m_Z^2}$. The model independent bound on kinetic mixing when $m_{Z'} = 30$ GeV is $\varepsilon \lesssim 0.03$ [12]. In the small ε limit,

$$\sin\xi = 0.62\varepsilon + \mathcal{O}(\varepsilon^3), \tag{7}$$

$$\cos\xi = 1 - 0.2\varepsilon^2 + \mathcal{O}(\varepsilon^4). \tag{8}$$

so we get $C_{ZZ'\phi} \sim (3.04 g' Y'_\phi + 20.87 \sin\alpha)\varepsilon$ GeV. Taking $\varepsilon = 0.03$ and $\sin\alpha = 0.2$, we find that $g' Y'_\phi$ should be at least ~ 1.3 in order to have $\Gamma(Z \to Z'\phi) \gtrsim 1.8 \times 10^{-5}$ GeV. Since $g' \lesssim 0.02$ from $Z \to 4\mu$ constraint, $Y'_\phi \gtrsim 65$ is required. Again, we find that a large Y'_ϕ is required in order to accommodate with the ALEPH dimuon excess.

V. CONCLUSIONS

In this letter we considered three different types of simplified models for the ALEPH 30 GeV dimuon excess in $Z \to b\bar{b}\mu^+\mu^-$. The first class of models where a new resonance couples to $b\bar{b}$ and $\mu^+\mu^-$ are basically ruled out by the DY production of dimuon through $b\bar{b} \to X \to \mu^+\mu^-$. In order to avoid the strong constraint from this DY process, we considered the second model where the 30 GeV dimuon excess is a spin-1 vector boson Z' and proposed a new vectorlike singlet quark B, which has nonzero couplings for Z-b-B and Z'-b-B. Then we could account for the ALEPH data without conflict with the DY constraint. One can test this model at the LHC by BB, Bb and Bj (with $j \neq b$) productions. The subsequent decay of B quark will result in the following final states: $bb + 4\mu$, $bj + 2\mu$ and $bb + 2\mu$, respectively, with $O(\text{nb}), O(\text{pb})$, as summarized in Tables III and IV. These B-quark production cross sections are sensitive to the B-quark mass m_B, and the current/future experimental studies of these channels will shed light on this class of models. Since the multi-muon final states have low background and rarely seen at the LHC, this scenario is likely to be excluded already although there is no explicit search for these final states. Finally we considered a new $U(1)'$ gauge symmetry which is spontaneously broken by a nonzero VEV of a singlet scalar ϕ which has nonzero $U(1)_Y$ and $U(1)'$ charges. Then there appears a nonzero vertex for Z-Z'-ϕ which can accommodate Eq. (1) through $Z \to Z'\phi \to bb\mu\mu$. A natural choice for $U(1)'$ would be $U(1)_{L_\mu - L_\tau}$ gauge symmetry. For both simplified models II and III, the model building issue will be nontrivial, since we need to introduce a new gauge symmetry associated with Z', most likely with flavor dependence, and the simplest gauge symmetry might be $U(1)_{L_\mu - L_\tau}$ gauge symmetry. In the model III, we considered the case where ϕ is an $SU(2)_L$ singlet case, and found that the $U(1)'$ charge of ϕ should be very large $\sim O(10^4)$ (or $O(10^2)$ for the model with the kinetic mixing). The case ϕ being an $SU(2)_L$ doublet or higher representation is beyond the scope of this letter. We hope to address it in separate publications in the near future.

Acknowledgments

We are grateful to Suyong Choi. Jack Kai-Feng Chen, Philip Coleman Harris and K.C. Kong for useful comments on the subject presented in this letter. This work is sup-

ported in part by National Research Foundation of Korea (NRF) Research Grant NRF-2015R1A2A1A05001869 (PK, JL, CY), and by the NRF grant funded by the Korea government (MSIP) (No. 2009-0083526) through Korea Neutrino Research Center at Seoul National University (PK). The work of CY is in part supported by the Do-Yak project of NRF under Contract No. NRF-2015R1A2A1A15054533.

[1] A. Heister, arXiv:1610.06536 [hep-ex].
[2] J. Alwall *et al.*, JHEP **1407**, 079 (2014) [arXiv:1405.0301 [hep-ph]].
[3] P. Ko, Y. Omura and C. Yu, Phys. Rev. D **85**, 115010 (2012) [arXiv:1108.0350 [hep-ph]]; JHEP **1201**, 147 (2012) [arXiv:1108.4005 [hep-ph]].
[4] K.A. Olive *et al.* (Particle Data Group), Chin. Phys. C, 38, 090001 (2014).
[5] S. Chatrchyan *et al.* [CMS Collaboration], JHEP **1212**, 034 (2012) [arXiv:1210.3844 [hep-ex]]; CMS Collaboration, CMS PAS SMP-16-009; G. Aad *et al.* [ATLAS Collaboration], Phys. Rev. Lett. **112**, no. 23, 231806 (2014) [arXiv:1403.5657 [hep-ex]].
[6] W. Altmannshofer, S. Gori, M. Pospelov and I. Yavin, Phys. Rev. Lett. **113**, 091801 (2014) [arXiv:1406.2332 [hep-ph]].
[7] CMS Collaboration, CMS-PAS-SMP-16-009.
[8] J. A. Aguilar-Saavedra, R. Benbrik, S. Heinemeyer and M. Prez-Victoria, Phys. Rev. D **88**, no. 9, 094010 (2013) [arXiv:1306.0572 [hep-ph]].
[9] The authors thank Suyong Choi and by Jack Kai-Feng Chen, Philip Coleman Harris and K.C. Kong for pointing this out to them.
[10] K. Cheung, P. Ko, J. S. Lee and P. Y. Tseng, JHEP **1510**, 057 (2015) [arXiv:1507.06158 [hep-ph]].
[11] G. Dupuis, JHEP **1607**, 008 (2016) [arXiv:1604.04552 [hep-ph]].
[12] A. Hook, E. Izaguirre and J. G. Wacker, Adv. High Energy Phys. **2011**, 859762 (2011) [arXiv:1006.0973 [hep-ph]].
[13] Y. Hochberg, E. Kuflik and H. Murayama, JHEP **1605**, 090 (2016) [arXiv:1512.07917 [hep-ph]].
[14] H. S. Lee and S. Yun, Phys. Rev. D **93**, no. 11, 115028 (2016) [arXiv:1604.01213 [hep-ph]].